

Quantum black holes with charge, colour, and spin at the LHC

Douglas M. Gingrich*

*Centre for Particle Physics, Department of Physics, University of Alberta,
Edmonton, AB T6G 2G7 Canada
E-mail: gingrich@ualberta.ca*

ABSTRACT: In low-scale gravity scenarios, quantum black holes could be produced at the Large Hadron Collider (LHC) provided the Planck scale is not higher than a few TeV. Based on fundamental principles and a few basic assumptions, we have constructed a model for quantum black hole production and decay in proton-proton collisions. By performing a detailed particle-level simulation at LHC energies, we have estimated cross sections and branching fractions for final-state particle topologies that would uniquely identify quantum black holes in LHC detectors. If the Planck scale is about a TeV, even with the most pessimistic assumptions, the rates for quantum black hole production are estimated to be above backgrounds, and some of the final-particle states are not found in Standard Model processes. Our results could form the starting point for a detailed investigation of quantum black holes by the LHC experiments.

KEYWORDS: black holes, extra dimensions, quantum gravity, beyond Standard Model.

*Also at TRIUMF, Vancouver, BC V6T 2A3 Canada.

Contents

1. Introduction	1
2. Quantum black hole states	2
3. Production of quantum black holes	3
4. Quantum black hole decay	8
5. Results	13
6. Summary	17

1. Introduction

Models of low-scale gravity [1, 2, 3, 4, 5, 6] allow for the production of small black holes in particle collisions [7, 8, 9]. The available energy must be well above the fundamental Planck scale for the semiclassical description of black hole production and decay to be valid. Based on current experimental and phenomenological limits on the Planck scale [10, 11, 12, 13, 14, 15, 16, 17, 18, 19, 20, 21, 22, 23, 24, 25], it is unlikely that semiclassical black holes will be accessible at energies produced by the Large Hadron Collider (LHC). However, if the Planck scale is low enough, quantum black holes may be produced in abundance at the LHC [9, 26, 27, 28].

In spite of not having a complete theory of quantum gravity, it is still possible to gain insight into the signatures of quantum black holes at the LHC based on some fundamental principles and a few assumptions [29]. The current thinking is that a black hole is formed if two partons from a proton-proton collision at the LHC satisfy the hoop conjecture [30]. It is natural for the local gauge symmetries of QCD colour and electric charge to be conserved during the black hole formation and decay processes [28]. The black hole thus inherits the colour, charge, and angular momentum from the parton pair that formed it. Hence, black holes can be characterized by QCD colour, electric charge, and angular momentum at the LHC.

Quantum black holes are expected to differ from semiclassical black holes in a number of ways. Semiclassical black holes are thought to decay thermally at the Hawking temperature and be well described by black hole thermodynamics. This is unlikely to be true for quantum black holes produced near threshold. We will consider black holes produced with mass just above the Planck scale. Since the decays are not thermal, we might expect quantum black hole decays into only a few-particle final states to dominate. The formation

and decay will occur over a small region of spacetime, and the quantum black hole might be viewed as a strongly coupled resonance or a gravitationally bound state. Since the production and decay is a short distance processes, and the quantum black hole is likely to have colour, the QCD hadronization process would occur after the decay.

With this simplified picture of quantum black hole production and decay, we perform a detailed study of the decay signatures that might be expected at the LHC. Our work builds on Ref. [29, 28] where these ideas, to our knowledge, were first discussed. We explicitly consider only ADD type black holes. However, there is a range of mass scales for which almost flat five-dimensional space is an applicable metric for Randall-Sundrum type-1 black holes. Some novel signatures that do not often occur in other beyond the Standard Model physics scenarios will be examined. Another unique feature is that, if black holds are produced, these signatures will occur at huge rates when compared to, even, Standard Model processes. With the startup of the LHC, such detailed phenomenological studies are of interest and of value.

This paper is structured as follows. In Sec. 2, we consider the electric charge, QCD colour, and spin of black holes produced in proton-proton collisions. A model for the production of quantum black holes at the LHC is discussed in Sec. 3 and their decays in Sec. 4. In Sec. 5, we estimate cross sections and discuss the topologies that might be observed in experiments.

2. Quantum black hole states

Quantum black holes can be classified according to their $SU(3)_c$ and $U(1)_{em}$ representations. Since we are considering proton-proton collisions, the allowed particles forming the black hole are quarks, antiquarks, and gluons. Nine possible electric charge states can be formed: $\pm 4/3, \pm 1, \pm 2/3, \pm 1/3, 0$. The $\pm 4/3$ and ± 1 charge states can only be formed by quark pairs, the charge states $\pm 2/3$ and $\pm 1/3$ can be formed by either two quarks, or a quark and a gluon, while the 0 charge state can be formed by either a quark-antiquark or pair of gluons.

The possible colour states of two partons are

$$3 \otimes \bar{3} = 8 \oplus 1 \quad (2.1)$$

$$3 \otimes 3 = 6 \oplus \bar{3} \quad (2.2)$$

$$\bar{3} \otimes \bar{3} = \bar{6} \oplus 3 \quad (2.3)$$

$$3 \otimes 8 = 3 \oplus \bar{6} \oplus 15 \quad (2.4)$$

$$\bar{3} \otimes 8 = \bar{3} \oplus 6 \oplus \bar{15} \quad (2.5)$$

$$8 \otimes 8 = 1_S \oplus 8_S \oplus 8_A \oplus 10 \oplus \bar{10}_A \oplus 27_S. \quad (2.6)$$

Since black holes form representations of $SU(3)_c$, they are predominantly coloured, but can occur as colourless singlets. Table 1 lists the possible charge and colour state combinations that could be produced. These states are not unique to quantum black holes but also apply to semiclassical black holes formed by two-parton collisions.

$QBH_{\bar{3}}^{4/3}$	$QBH_6^{4/3}$			
$QBH_{\bar{1}}^1$	QBH_8^1			
$QBH_{\bar{3}}^{2/3}$	$QBH_6^{2/3}$	$QBH_{15}^{2/3}$		
$QBH_{\bar{3}}^{1/3}$	$QBH_6^{1/3}$	$QBH_{15}^{1/3}$		
$QBH_{\bar{1}}^0$	QBH_8^0	QBH_{10}^0	QBH_{10}^0	QBH_{27}^0

Table 1: Possible quantum black hole states of different electric charge (superscript) and colour representation (subscript). For the charged states, there are a corresponding 10 states of opposite charge which are not shown.

At energies of the fundamental Planck scale M_D , the size in spacetime of the incoming partons and the gravitational radius r_g of the black hole are both of order M_D^{-1} . Since the impact parameter is of the same size as the gravitational radius, the angular momentum of the two-particle system, $J \leq Mr_g$, would be of order unity. Thus, a possible semiclassical black hole spin-down process is unlikely to apply to quantum black holes. This statement relies on the hoop conjecture of classical gravity being applicable in the strong gravity regime.

For simplicity, we will consider the initial angular momentum of the quantum black hole to be due entirely to the spin states of the incoming partons, and ignore the possibility of an initial small orbital angular momentum due to an impact parameter. When considering spin states, we will assume massless partons. Since we are ignoring angular momentum (transverse to the helicity axis), the quantum black hole spin will be parallel to the parton helicity axis, or the beam axis at the LHC. This is quite different from semiclassical black holes with angular momentum. In this case, the convention is to add the small amount of spin angular momentum to the normally larger orbital angular momentum, which is transverse to the helicity axis [31]. The quark-quark states can form spin-0 and spin-1 quantum black holes. The spin-1 state is three times more likely to form than the spin-0 state. The quark-gluon states can form spin-3/2 and spin-1/2 quantum black holes. However, because the partons are massless, not all spin combinations are possible. The spin-3/2 state is twice as likely to form as the spin-1/2 state. The gluon-gluon states can form spin-0 and spin-2 quantum black holes. Again because the partons are massless, not all spin combinations are possible. The spin-1 state is not allowed and there are no ± 1 states along the spin axis in the spin-2 case. The spin-2 state is three times more likely to form than the spin-0 state.

3. Production of quantum black holes

The cross section for black hole production is not known. Based on classical arguments and only one available scale, the cross section is most often taken to be the geometrical cross section $\sigma \sim \pi r_g^2$, where r_g is the gravitational radius of the two-particle system (see Ref. [32] for a review). This cross section assumes a radiationless production process in which all the energy of the two-particle system goes into forming the black hole. Various calculations have been performed to predict the amount of gravitational radiation in the

production process, but for higher-dimensional gravity only the trapped surface approach has yielded numerical results [33, 34, 35]. The effect of radiation on the cross section is smallest for low black hole masses [32]. For the quantum black holes that we will consider, the trapped surface cross section is about 0.02 time less than the geometrical cross section. However, for higher-dimensions and non-zero impact parameter, these calculations can only be considered as lower bounds on the cross section. In addition, the calculations have ignored parton charge, parton spin, and parton finite size (see Ref. [36, 37, 38, 39] for progress in these areas). The calculations are based on classical arguments, and since it is not known how applicable these might be in the quantum regime, we will not consider them except for to realized that the cross sections might be lower by as much as about two orders of magnitude.

Arguments have been made for why the geometrical cross section, to within a small numerical coefficient, should be applicable to quantum black holes [40, 41]. Alternatively, if one embeds a quantum theory of gravity into string theory, the cross section is reduced due to the quantum size of the string [39]. The energy threshold for quantum black hole production would be somewhat larger than M_D by a factor that depends on the ratio of string length to Planck length, or the string coupling in weakly-coupled string theory. The amount of reduction in the cross section will remain unknown until these fundamental constants have been determined.

We assume the production cross section for quantum black holes can be extrapolated from the cross section for semiclassical black holes. It is a challenge for the experiments to measure or set a limit on the black hole cross section. This might be one of the few numerical quantities the experiments can address in an almost model independent way.

The gravitational radius r_g of a quantum black hole of mass M becomes

$$r_g = k(D) \frac{1}{M_D} \left(\frac{M}{M_D} \right)^{\frac{1}{D-3}}, \quad (3.1)$$

where D is the total number of spacetime dimensions, and $k(D)$ is a numerical coefficient depending only on the number of dimensions and the definition of the fundamental Planck scale; the PDG definition of the Planck scale is used in this study:

$$k(D) = \left(2^{D-4} \sqrt{\pi}^{D-7} \frac{\Gamma\left(\frac{D-1}{2}\right)}{D-2} \right)^{\frac{1}{D-3}}. \quad (3.2)$$

We now address the question of over what mass range is a black hole a quantum object? It is common to take the validity of the semiclassical black hole to be when the Compton wavelength of the colliding particles lies within the gravitational radius. We turn this condition around and consider it to be the upper mass bound for considering the black hole to be in the quantum regime. With this mass restriction, we stay away from the semiclassical regime, where black hole thermodynamics and thermal decays occur. This bound also ensure that the initial angular momentum of the quantum black hole is close to unity. If we do not take the upper mass requirement into account, the tails of distributions (particle momentum, for example) might be artificially altered due to semiclassical black

hole decays. We consider the lower mass, or threshold, to be when the mass of the black hole is equal to the inverse of its radius. Using the PDG convention for the Planck scale gives

$$\left(\frac{1}{k}\right)^{\frac{D-3}{D-2}} \lesssim \frac{M}{M_D} \lesssim \left(\frac{4\pi}{k}\right)^{\frac{D-3}{D-2}}. \quad (3.3)$$

We notice that the minimum mass is below the fundamental Planck scale. This is an artifact of the definition of the Planck scale. Using the more intuitive Dimopoulos-Landsberg definition of the Planck scale gives a minimum mass always above the fundamental Planck scale. On the other hand, the accelerator experiments have set limits on M_D of $M_D \gtrsim 1$ TeV, and hence a quantum black hole would be required to have mass above only about 500 GeV. If M_D is about 1 TeV, could it be that the Tevatron has failed to observe the effects of relatively low-mass black holes? Assuming this is not the case, we will take the threshold for quantum black hole production to be the Planck scale in the PDG definition, and consider a fixed mass range for all dimensions: $M_{\min} = M_D$ and $M_{\max} = 3M_D$.

Only a fraction of the total centre of mass energy \sqrt{s} in a proton-proton collision is available in the hard scattering process. We define $s x_a x_b \equiv s x_{\min} \equiv \hat{s}$, where x_a and x_b are the fractional energies of the two partons relative to the proton energies. The full particle-level cross section σ is given by

$$\sigma(QBH_{p_1 p_2}^q) = \sum_{a,b} \int_{M^2/s}^1 dx_{\min} \int_{x_{\min}}^1 \frac{dx}{x} f_a\left(\frac{x_{\min}}{x}\right) f_b(x) \pi k^2(D) r_g^2, \quad (3.4)$$

where a and b are the parton types in the two protons, and f_a and f_b are the parton distribution functions (PDFs) for the proton. The sum is over all the possible quark and gluon pairings that can make a particular quantum black hole state. The parton distributions fall rapidly at high relative energies, and so the particle-level cross section also falls at high energies.

When describing quantum black hole production, it will be more informative to specify the two partons p_1 and p_2 that went into the formation of the black hole, and drop the colour representation specifier by summing over the possible colour representations. This makes sense since the partons hadronize after the quantum black hole decays. The relative probabilities of each colour representation will be accounted for in the decay branching fractions. The resulting 14 different processes can be used to obtain any desired inclusive result by multiplying the cross section by the branching fraction and summing the relevant processes.

To obtain numerical results, we have used the parameters shown in Table 2. You may assume these parameters were used in calculations unless told otherwise. The CTEQ6L1 parton distribution functions [42] were used with a QCD scale of $Q = 1/r_g$. The cross section spectrum of quantum black hole states is shown in Fig. 1. It is interesting to note that the highest cross section is given by u - g collisions. This shows the importance of the gluon contribution at the parton kinematics and QCD scale that we are using. As expected, the inclusive cross section, of about 130 nb, is significantly higher than the semiclassical black hole cross section. This value should be considered as an upper limit.

Value	Symbol	Description
10	D	total number of spacetime dimensions
1 TeV	M_D	fundamental Planck scale (PDG definition)
14 TeV	\sqrt{s}	LHC centre of mass energy
M_D	M_{\min}	minimum quantum black hole mass
$\min(3M_D, \sqrt{s})$	M_{\max}	maximum quantum black hole mass

Table 2: Default parameters used in calculations.

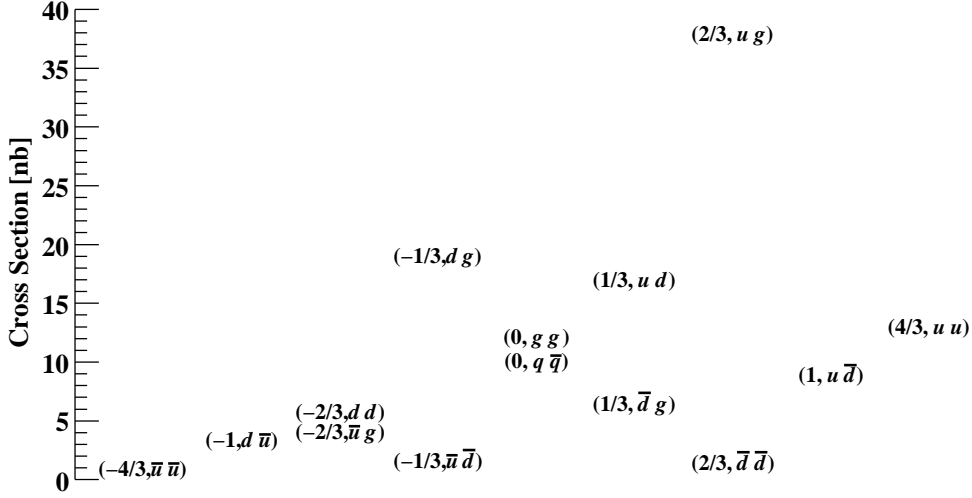


Figure 1: Cross section spectrum for quantum black holes of different electric charge and parton progenitors.

The cross section is sensitive to the choice of PDFs and QCD scale. Table 3 shows the inclusive quantum black hole cross section for four different choices of PDFs and two different QCD scales. A difference of about 7% is observed for the different PDFs. Our calculations use $Q = 1/r_g$ for the QCD scale. If $Q = M$ is used, the cross sections are about 13% lower.

Figure 2 shows how the total inclusive cross section changes with different number of dimensions and different values for the Planck scale. If the LHC detectors can collect a few hundred pb^{-1} of data in the first years, they will be able to produce significant numbers

QCD Scale	Parton Density Functions			
	CTEQ6L1	CTEQ5L	CTEQ5M	MRST98
$Q = 1/r_g$	132	136	159	150
$Q = M$	115	119	139	132

Table 3: Inclusive quantum black hole cross section in nanobarns for different parton density functions and different QCD scales.

of quantum black holes for Planck scales as high as about 5 TeV, if the geometrical cross section is valid. Also shown in Fig. 2 are the trapped surface lower-bound cross sections. These cross sections are about 10 to 10^4 lower than the geometrical cross section over the range $1 < M_D < 4$ TeV. In this case, we see that there is very little dependence on the number of dimensions. In calculating the trapped surface cross section, the quantum black hole mass has been limited to the range of $M_D < M < 3M_D$. That is, if the mass before gravitational radiation is above $3M_D$ it is not included in the total cross section calculation.

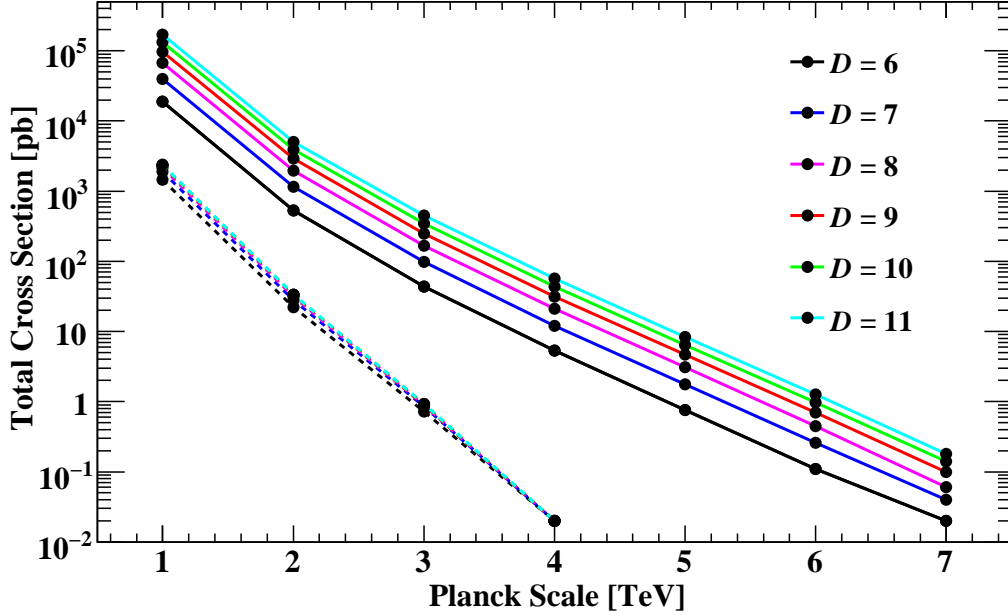


Figure 2: Total proton-proton cross section for different number of dimensions D and different fundamental Planck scales. The solid lines are totally inelastic cross sections and the dashed lines are trapped surface cross sections.

Because of the falling product of parton distribution functions with parton-parton centre of mass energy \sqrt{s} , the most probable value for the quantum black hole mass is M_D . At this value, the gravitational radius, and hence cross section, is independent of the quantum black hole mass. Thus the shape of the cross section at the lowest possible masses is almost independent of the parton cross section and is determined predominantly by the parton distribution functions. Since each quantum black hole state is made from unique valance quarks, sea quarks, or gluons, the product of parton density functions can be vary different. Figure 3 shows the mass distribution for two rather different quantum black hole states. Although gluons contribute the most at low masses, the u -quarks (valance quarks) contribute the most above masses of about $1.5M_D$. Over the mass region $1 < M < 3$ TeV, the $uu \rightarrow QBH^{4/3}$ differential cross section falls as a power law in the mass with exponent -2.1 , while the $gg \rightarrow QBH^0$ cross section falls as a power law in the mass with exponent -4.6 .

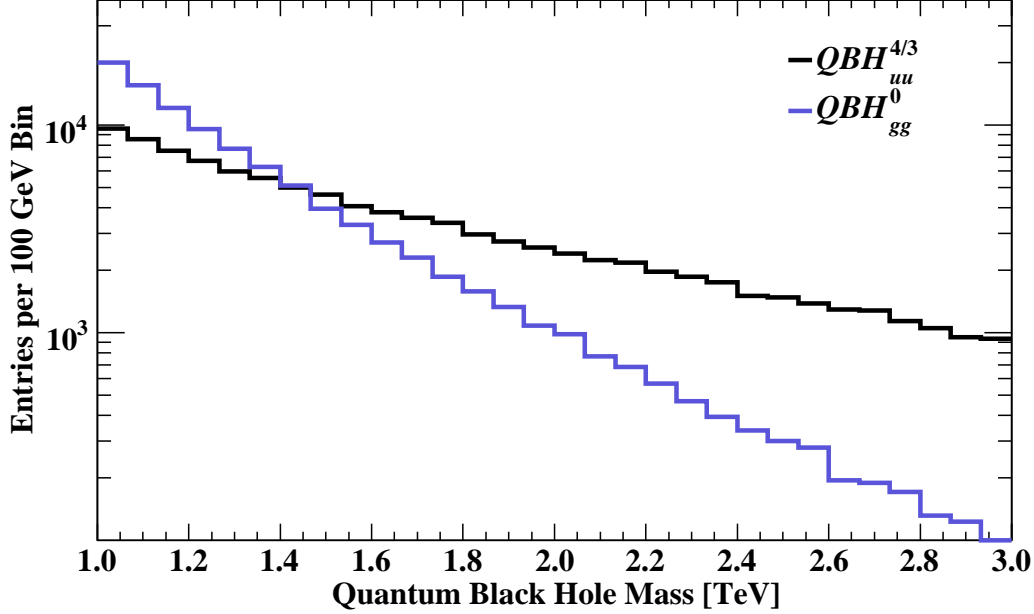


Figure 3: Quantum black hole mass distribution for two different quantum black hole states.

Since quantum black holes are predominantly produced near threshold, their kinematics are different from the kinematics of semiclassical black holes. Figure 4 shows the kinematics of quantum black holes. The mean mass is about $1.5M_D$, the mean energy is about $2M_D$, and the mean momentum is about $0.9M_D$. The distribution of values of the Lorentz variables β and γ can be easily explained. They depend only on the x_a and x_b values of the two partons forming the black hole, or equivalently on the \hat{s} and s values. β and γ are given by

$$\beta = \frac{|x_a - x_b|}{x_a + x_b} \quad \text{and} \quad \gamma = \frac{x_a + x_b}{2\sqrt{x_a x_b}}. \quad (3.5)$$

For symmetric collisions ($x_a \approx x_b$), $\beta \approx 0$ and $\gamma \approx 1$. For highly asymmetric collisions ($x_1 \approx 1$ and $x_2 \approx x_{\min}$),

$$\beta \approx \frac{|s - \hat{s}|}{s + \hat{s}} \approx 0.99 \quad \text{and} \quad \gamma \approx \frac{s + \hat{s}}{2\sqrt{s\hat{s}}} \approx \frac{\sqrt{s}}{2\sqrt{\hat{s}}} \approx \frac{E_{\text{beam}}}{2 \text{ TeV}} \approx 7. \quad (3.6)$$

Thus, based on Fig. 4 we can see that the collisions are more asymmetric than symmetric.

4. Quantum black hole decay

Up until now, we have visualized the hard scattering process as occurring through a quantum black hole resonance; in analogy to a particle resonance. It is informative to estimate the width of this possible resonance. For a well defined resonance, we will use the criteria

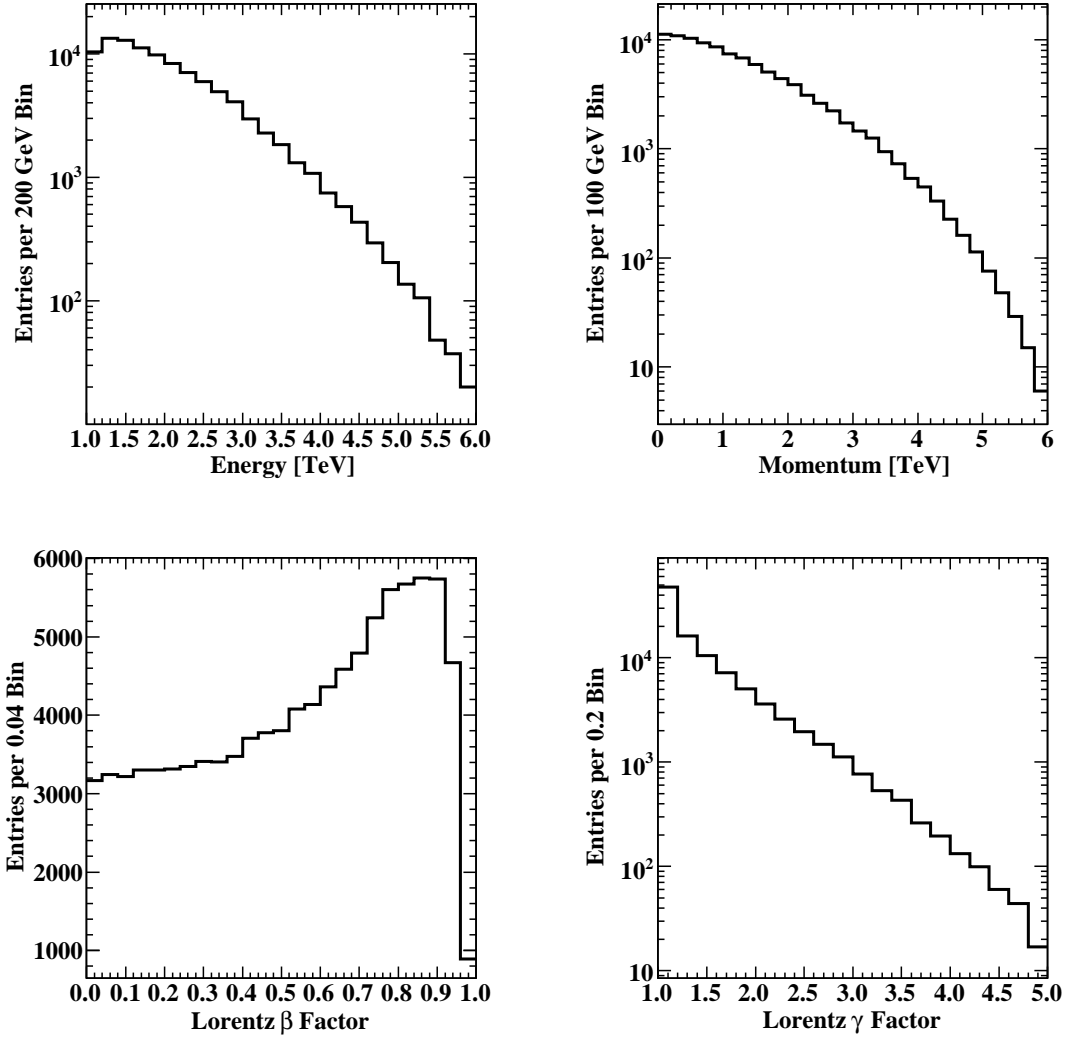


Figure 4: Distributions of some kinematic variables of quantum black holes.

that $\tau \gg 1/M$, where M is the initial quantum black hole mass and τ is its lifetime. It is assumed that the quantum black hole decays entirely without leaving a remnant. When estimating the lifetime, it is usual to assume Hawking emission of massless particles during the entire decay process. One can start with the power spectrum for black hole emission or go directly to the generalized Stefan-Boltzmann equation and relate the Hawking temperature to the Schwarzschild radius. The total power emitted will be equal to the rate of decrease of the black hole mass. The resulting differential equation is then integrated over the entire lifetime of the black hole and the result is given by

$$\tau = \frac{1}{CM} \left(\frac{M}{M_D} \right)^{\frac{2(D-2)}{D-3}}, \quad (4.1)$$

where the form of C depends on how the emissivities of the different fields are normalized. In any case, C involves a sum over the particle degrees of freedom for each spin weighted by the integrated power emitted into each spin field. The power factors are greybody-modified thermal power spectra proposed by Hawking [43].

Since we are considering non-thermal quantum black hole decays, the applicability of Eq. (4.1) is questionable. However, we will consider it as an indicative estimate of the quantum black hole lifetime. Since quantum black holes are produced with mass close to the Planck scale, we expect $\tau M \gtrsim 1/C$. Thus our requirement for a resonance translates into $C \ll 1$ or large mass (at which point the black hole is semiclassical). The coefficient C increases with the number of particle degrees of freedom, the value of the greybody factors, and the number of dimensions. If greybody factors are ignored, $C \approx 2$ for $D = 10$ and does not drop below unity until $D < 8$. If we use greybody factors calculated according to Ref. [44] and only consider emission on the brane, $C \approx 5$ for $D = 10$, and C is still greater than two for seven dimensions. If we include the emission of gravitons into the bulk [45], the number of degrees of freedom increases, particularly for higher dimensions, and C becomes even larger. Thus, unless we push the limits of the quantum black hole mass into the semiclassical regime or restrict our considerations to low number of extra dimensions (those likely to be excluded by experiments), a quantum black hole probably can not be viewed as a particle resonance. Some authors have reached similar conclusions [46, 29]. The concept of a quantum black hole state still has the useful purpose of labeling the possible interactions.

In the decays of quantum black holes, one expects the number of particles in the final state to be small. Using arguments similar to those used to estimate the lifetime, the average number of particles emitted from the black hole during Hawking evaporation can be estimated to be

$$\langle N \rangle = \rho S \sim \left(\frac{M}{M_D} \right)^{\frac{D-2}{D-3}}, \quad (4.2)$$

where S is the initial entropy. The form of ρ depends on how the emissivities of the different fields are normalized. If greybody factors are ignored, the average multiplicity is between 1.0 to 1.3 for 6 to 10 dimensions. If greybody factors are included and emission is restricted to the brane, there is no significant change in the average multiplicities. Allowing graviton emission into the bulk gives the numbers shown in the second column of Table 4. The mean multiplicity increases with the number of dimensions to a maximum for nine dimensions and then decreases. This is due to the interplay between the entropy definition (due to the Planck scale definition) and the ratio of the sum of fluxes to sum of powers in the coefficient ρ in Eq. (4.2).

Fluctuations about the mean multiplicity can be described using a Poisson distribution [47, 25]. The Poisson distribution can also be used to estimate the relative probabilities of two-particle, three-particle, four-particle, etc. final states. When calculating the relative probabilities, we have removed the case of zero particle emission and renormalized the Poisson distributions. We consider single-particle emission to represent two-particle decay in that the remaining black hole is considered to be the second particle. Using these

concepts, the probabilities for different number of particles in the final state are shown in Table 4. For $D = 7$ to 11 there is little dependence on the number of dimensions. Approximately 50% of the decays are two-particle, while three-particle and four-particle decays are not insignificant. The multiplicities depend on the definition of the Planck scale. For the Dimopoulos-Landsberg definition and the case of $D = 10$, the mean multiplicity is 0.4 and the probability of a two-particle decay is about 80%. The two-particle state is enhanced because, by using a different definition of the Planck scale, we are effectively considering a lower threshold for quantum black hole production. In what follows, we will only consider two-particle final states. Clearly, an extended analysis should include higher multiplicity decays.

D	$\langle N \rangle$	Number of Particles				
		2	3	4	5	6
5	0.6	0.74	0.21	0.04	0.01	0.00
6	0.9	0.61	0.28	0.09	0.02	0.00
7	1.1	0.54	0.30	0.11	0.03	0.01
8	1.2	0.51	0.31	0.13	0.04	0.01
9	1.3	0.50	0.31	0.13	0.04	0.01
10	1.2	0.51	0.31	0.13	0.04	0.01
11	1.1	0.54	0.30	0.11	0.03	0.01

Table 4: Mean number of emissions $\langle N \rangle$ and probability of each number of particles in the final state versus the number of dimensions D .

$M_D/2$. Most particles will remain in a detector and are highly relativistic.

In quantum black hole decays, we consider the colour and charge to be conserved, but make no similar assumptions about global charges like baryon or lepton number. We consider gravity to be totally democratic and couple to all flavours of quarks, leptons, and gauge bosons equally. Although perhaps debatable, we assume Lorentz invariance holds, and only allow decays that conserve total angular momentum.

Experimental bounds on the effects of higher-dimension operators might limit the parameter space over which we can consider decays violating global charges. The limits on flavour-changing lepton decays and proton decay should be taken into consideration. Unfortunately, it is not clear what the relationship is between the Planck scale and the scale occurring in higher-dimension operators. Arguments have been made for why the experimental constraints are serious but do not necessarily rule out the allow parameter space that we will consider [29, 28]. It is also possible that the global symmetries may be gauged.

Quantum black holes have colour and size of about $M_D^{-1} \lesssim 1 \text{ TeV}^{-1}$. The decay products can be partons in coloured representations, which can travel a distance of about the QCD scale of a Fermi before they have to hadronize to form colour singlets. Thus, we only allow parton decay final states that can have the colour representation of the quantum black hole, or equivalently, the colour representation of the initial parton progenitors. Since it would be difficult to identify the quantum black hole colour in experiments, we will

For the decay kinematics, we have used two-particle phase space decays. The decay particle kinematics are shown in Fig. 5. In the Lorentz β and γ distributions, we have excluded zero-mass particles and low-mass particles: electrons, muons, u -quarks, and d -quarks. Since we are using two-particle decays, the distributions are representative of all particle types, except for the distributions of the Lorentz variables β and γ . The most probable particle energy, momentum, or transverse momentum is about

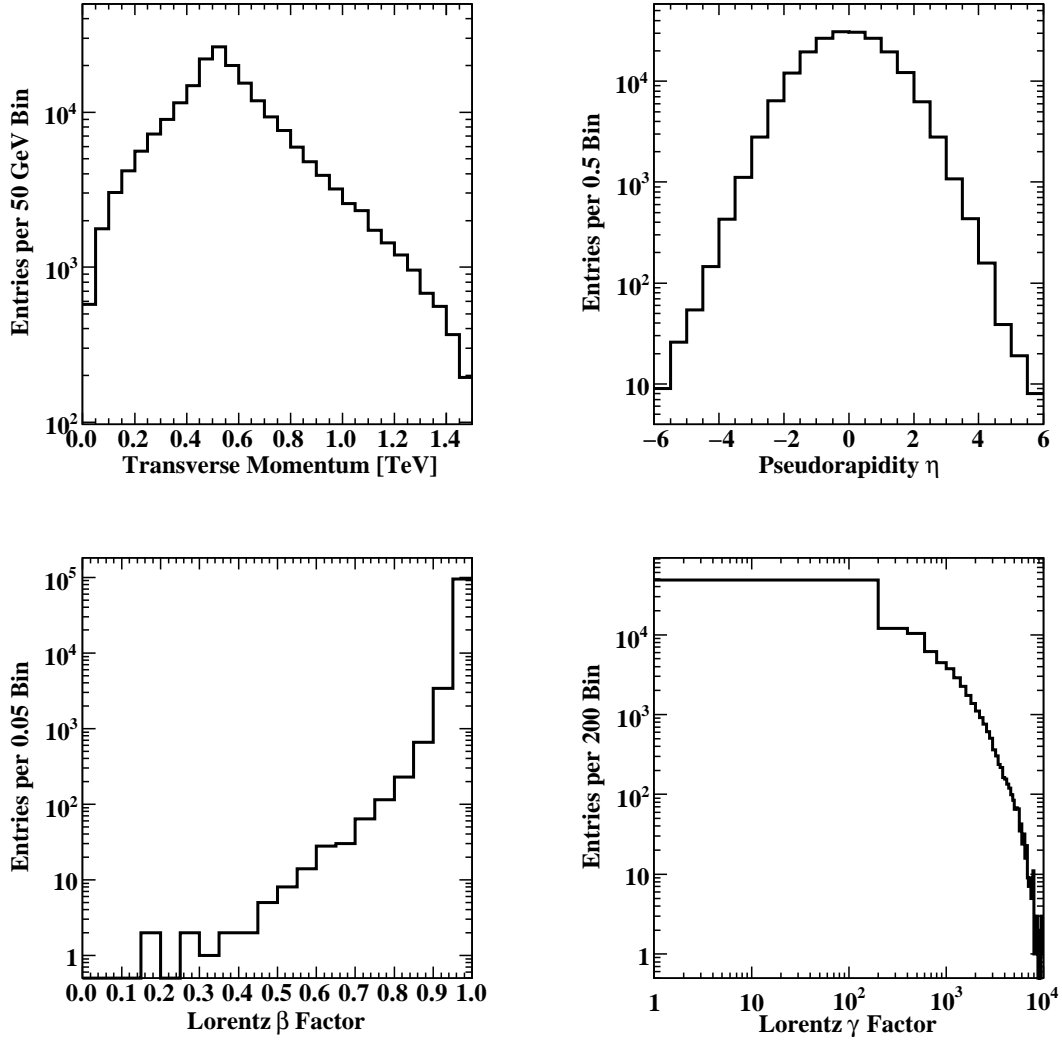


Figure 5: Distributions of some kinematic variables for decay particles from quantum black holes. Massless particles, electrons, muons, u -quarks, and d -quarks have not been included in the Lorentz β and γ distributions.

consider the different singlet and octet representations (see Eq. (2.1) and (2.6)) to be the same when counting the number of degrees of freedom.

The particle content of low-scale gravity is uncertain. A Higgs boson might be discovered and there is likely to be a graviton. In addition, how the neutrino sector couples to gravity is an interesting topic. Now that at least one neutrino has mass, it is possible that gravity will couple to neutrinos of both left- and right-handedness equally. In addition, whether neutrinos are Dirac or Majorana particles will change the number of available final states. However, the biggest factor effecting the final state particles is if the global symmetries of the Standard Model remain good symmetries at the strong gravity scale. In

presenting our results, we most often consider two extreme particle content models. Our base model allows global symmetries to be violated, includes a Higgs and graviton, and assumes the neutrinos are Majorana particles of both handedness. Our comparison model is the currently observed Standard Model: global symmetries are conserved, there is no Higgs or graviton, and the neutrinos are left-handed Dirac particles. When considering the different particle content models it is important to realize that coupling per degree of freedom in Hawking radiation does not apply in the quantum gravity cases. For quantum gravity, we are simply assuming the coupling to all quark and lepton flavours are equal.

We determined the branching fractions for each quantum black hole state as follows. For each state, we wrote down all the two-particle final states that could conserve colour, charge, and angular momentum. Some decay states can not conserve all the angular momentum modes and were thus weighted accordingly. For each decay mode, we formed a product of weights given by the number of members in the colour representation, times the number of flavour combinations, times the spin degrees of freedom. The decay branching fractions are shown Table 5.

5. Results

Using the previously developed model, we have simulated the production and decay of quantum black hole events, with each state weighted by its cross section, using a new Monte Carlo event generator described in Ref. [48]. The particle PDG identifier codes for the two decay particles in the hard scattering are shown in Fig. 6. We notice the expected dominance of quarks and gluons, and the charge and baryon asymmetry from having two protons collide, rather than a proton-antiproton collision. Figure 6 is for the observed Standard Model particle content and can look significantly different depending on the particle content model. If neutrinos are chiral, the number of charged leptons and neutrinos are approximately equal. If global symmetries can be violated, the number of charged antileptons and antineutrinos increases, while the number of antiquarks decreases. Including the graviton is significant, while the Higgs boson has little effect. Figure 7 show the frequency of particle identification codes when including all these effects. We notice a significant increase in leptons and near equality between the different antiquark flavours.

We have studied the multiplicities of various particle signatures in a detector: jets, electrons, muons, photons, and missing energy. For this calculation, we allowed the t , W , Z , and H to decay. We called all quarks, gluons, and tau particles jets. On average per event there are 2.4 jets, 0.05 electrons, 0.05 muons, 0.05 photons, and 0.2 particles (neutrinos and gravitons) that give missing energy. There is very little variation due to changing the particle content model. If global symmetries can be violated, the average number of electrons, muons, and particles giving missing energy per event are marginally higher. This is because of the domination of jets in both cases.

It is useful to know the average number of jets in events and how the decays of the t -quark, W , and Z effect these numbers: 99% of the events have at least one jet, 88% of the event at least two jets, and 28% of the events at least three jets. If global symmetries are violated, the number of events with two or more jets decreases by about 10%. Parton

State	Decay	BR (%)		State	Decay	BR (%)	
		C	V			C	V
$QBH_{uu}^{4/3}$	$\rightarrow uu$ $\bar{d}\ell^+$	100	67 33	$QBH_{q\bar{q}}^0$	$\rightarrow u\bar{u}$ $d\bar{d}$ gZ gg $g\gamma$ $\ell^+\ell^-$ $\nu\nu$ W^+W^- $\gamma\gamma$ ZZ γZ gH γH ZH HH gG γG ZG GG	45.1 45.1 3.3 1.1 1.1 1.7 0.8 0.6 0.1 0.6 0.4 2.0 0.3 0.5 0.1 2.0 0.2 0.2 0.1	40.3 40.3 3.0 1.0 1.0 4.5 3.0 0.5 0.1 0.5 0.4 2.0 0.3 0.5 0.1 2.0 0.2 0.2 0.1
$QBH_{u\bar{d}}^1$	$\rightarrow u\bar{d}$ $\nu\ell^+$ W^+g W^+Z $W^+\gamma$ W^+H W^+G	88 3 7 1 1	81.6 9.1 6.0 1.0 0.8 1.0 0.5	$QBH_{ug}^{2/3}$	$\rightarrow ug$ dW^+ $u\gamma$ uZ uH uG	73 9 9 9	67.6 8.5 8.5 8.5 2.8 4.2
$QBH_{d\bar{d}}^{2/3}$	$\rightarrow d\bar{d}$ $u\nu$ $d\ell^+$	100	50 25 25	$QBH_{dg}^{1/3}$	$\rightarrow \bar{d}g$ $\bar{u}W^+$ $\bar{d}\gamma$ $\bar{d}Z$ $\bar{d}H$ $\bar{d}G$	73 9 9 9	67.6 8.5 8.5 8.5 2.8 4.2
$QBH_{ud}^{1/3}$	$\rightarrow ud$ $\bar{d}\nu$ $\bar{u}\ell^+$	100	60 20 20	QBH_{gg}^0	$\rightarrow u\bar{u}$ $d\bar{d}$ gg gZ $g\gamma$ $\ell^+\ell^-$ $\nu\nu$ W^+W^- $\gamma\gamma$ ZZ γZ ZH HH HG GG	23.1 23.1 38.7 9.7 2.4 0.5 0.6 0.6 0.6 0.6 0.1 0.1 0.4 0.3	22.5 22.5 37.6 9.4 2.4 1.3 0.9 0.6 0.6 0.6 0.1 0.1 0.4 0.3

Table 5: Quantum black hole decay branching fractions. BR is the branching fraction, C means global symmetries are conserved and V means they may be violated.

hadronization, detector effects, and jet-finding algorithms will cause the number of jets per event to be higher.

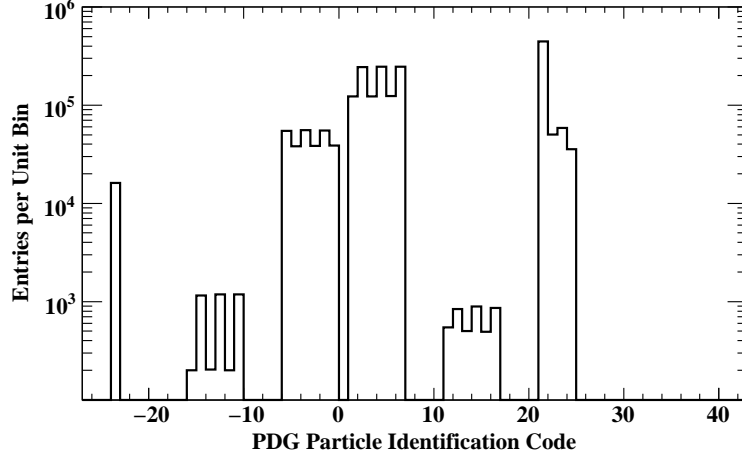


Figure 6: Relative occurrence of decay particle types according to their PDG identification code. Observed Standard Model particle content with global symmetries conserved.

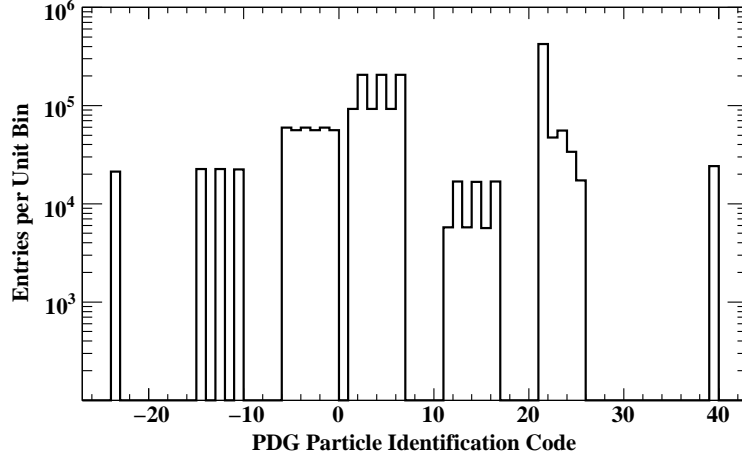


Figure 7: Relative occurrence of decay particle types according to their PDG identification code. Global symmetries may be violated, neutrinos are chiral and Majorana, and a Higgs and graviton are allowed.

To study the topologies of the events, we do not allow the final-state particles to decay. The percentage occurrence of each topology is shown in Table 6. As expected, di-jet events dominate. Also significant are mono-jet, jet plus t -quark, jet plus gauge-boson, and jet plus lepton topologies. Noteworthy is the electron plus muon topology at the 0.1% level. Such a signal is not usually produced in other beyond the Standard Model physics processes. The cross sections are also shown in Table 6, along with predictions of the Standard Model when using PYTHIA 8 [49, 50]. For the Standard Model processes, we have restricted the phase-space by requiring the invariant mass to be between 1 TeV and 3 TeV, and the transverse momentum in the rest frame of the hard scattering process to be between 500 GeV and 1.5 TeV. In most cases, the Standard Model cross sections are more than

three orders of magnitude lower. So even if the quantum black hole cross sections are at the lower bound given by the trapped surface calculation, the number of events produced in each decay topology should be greater than the Standard Model background.

Topology	B, L Conserved		B, L Violated		Standard Model
	(%)	σ (pb)	(%)	σ (pb)	σ (pb)
di-jets	66	8.7×10^4	57	7.5×10^4	630
jet + t	16	2.1×10^4	12	1.6×10^4	1.4
jet + Z	5.5	7.3×10^3	5.2	6.9×10^3	1.2
jet + W	4.9	6.5×10^3	5.1	6.8×10^3	2.8
jet + γ	4.8	6.4×10^3	4.4	5.8×10^3	8.9×10^{-1}
$t\bar{t}$	2.2	2.9×10^3	1.8	2.4×10^3	1.7×10^{-1}
mono-jets	0.067	89	6.2	8.2×10^3	
jet + μ			2.4	3.2×10^3	
jet + e			2.4	3.2×10^3	
jet + H			1.5	2.0×10^3	
no energy	0.061	81	0.33	440	
mono- μ	0.069	92	0.25	330	
mono- e	0.064	85	0.25	330	
di- Z	0.092	120	0.087	120	5.2×10^{-3}
di- W	0.091	120	0.087	110	2.7×10^{-2}
$Z + W$	0.066	88	0.081	110	1.0×10^{-2}
di- γ	0.065	86	0.057	92	2.2×10^{-3}
γ - Z	0.076	100	0.077	100	4.1×10^{-3}
γ - W	0.046	61	0.059	78	2.8×10^{-3}
di- μ	0.050	66	0.048	64	
di- e	0.055	73	0.047	63	
$e + \mu$			0.096	140	
$W + H$			0.078	110	2.6×10^{-3}
$Z + H$			0.046	61	1.3×10^{-3}
mono- W			0.040	53	1.5×10^{-1}
mono- H			0.034	45	1.5×10^{-4}
mono- Z			0.019	25	6.3×10^{-2}
mono- γ			0.018	24	2.9×10^{-2}
$H + H$			0.022	29	
H - γ			0.019	26	

Table 6: Percentage occurrence and cross section for each decay topology. Columns two and three are for quantum black holes that conserve global symmetries and columns four and five are for quantum black holes that may violate global symmetries. The last column is for Standard Model QCD and electroweak processes.

The previous analysis used a Planck scale of 1 TeV, which is a hard lower bound for $D > 6$. If one considers how Kaluza-Klein gravitons would affect supernovae cooling

and neutron stars, the lower bounds on the Planck scale are higher [18, 19]. However, it should be realized that the bounds provided by astrophysical arguments contain significant uncertainties, such as the compactification moduli. For $D < 8$, the lower bound on the fundamental Planck scale is too high to allow quantum black holes to be produced by the LHC. For higher dimensions, the bounds on the Planck scale are less stringent. For $D = 8$, $M_D > 4$ TeV and for $D > 8$, $M_D > 1.4$ TeV. For $D > 8$, the lower bound on the Planck scale is set by the absence of black holes in neutrino cosmic ray showers [25]. Using the results of Fig. 2, we see that for $D = 8$, $\sigma \sim 20$ pb and for $D > 8$, $\sigma \gtrsim 2 \times 10^4$ pb. Thus, most decay signatures in Table 6 would be observable for $D > 8$, while probably none would be observable for $D < 8$.

We comment on the $D = 8$ case a little more by giving some order of magnitude estimates. We assume the ratio of the number of observed events to the experimental acceptance is 10^3 . For di-jet events, the over all acceptance might be high, but some background can be anticipated and hence on the order of 100 events will need to be observed. While in the case of leptons, the backgrounds might be lower, but the acceptance will probably be lower since more stringent requirements might be needed to reduce lepton fake rates, and ensure the leptons are not accompanied by additional jets. Thus about 80 pb^{-1} of data would be required to see an anomaly in the Standard Model di-jet events, and about 1 fb^{-1} to see one in a jet plus lepton signal. About 50 fb^{-1} of data would be needed for a definitive statement to be made in the electron plus muon channel.

6. Summary

We have considered black hole production and decay near the Planck scale. Based on fundamental principles and some assumptions, we have built a model to estimate cross sections and decay topologies. Although di-jet decays denominate, they are unlikely to be the only decays with a significant rate. The jet plus gauge-boson and jet plus t -quark topologies account for about 30% of the decays. In models where global symmetries need not be conserved, jets plus leptons and mono-jets are also significant decays. If the Planck scale is low enough so that the inclusive cross section is of the order of 100 nb, then even the decays with low branching fractions will be readily observable. Signatures such as opposite sign electron plus muon, with very little else in the detector, will be hard to explain by conventional physics. Observing anomalous rates in several of the decay channels could help determine the nature of the new physics and lead to the discovery of quantum gravity.

Acknowledgments

I would like to thank Xavier Calmet and De-Chang Dai for helpful e-mail discussions. This work was supported in part by the Natural Sciences and Engineering Research Council of Canada.

References

- [1] N. Arkani-Hamed, S. Dimopoulos, and G. Dvali, *The hierarchy problem and new dimensions at a millimeter*, *Phys. Lett. B* **429** (1998) 263–272, [[arXiv:hep-ph/9803315v1](#)].
- [2] I. Antoniadis, N. Arkani-Hamed, S. Dimopoulos, and G. Dvali, *New dimensions at a millimeter to a fermi and superstrings at a TeV*, *Phys. Lett. B* **436** (1998) 257–263, [[arXiv:hep-ph/9804398v1](#)].
- [3] L. Randall and R. Sundrum, *Large mass hierarchy from a small extra dimension*, *Phys. Rev. Lett.* **83** (1999) 3370, [[arXiv:hep-th/9905221v1](#)].
- [4] L. Randall and R. Sundrum, *An alternative to compactification*, *Phys. Rev. Lett.* **83** (1999) 4690, [[arXiv:hep-th/9906064v1](#)].
- [5] X. Calmet and S. D. H. Hsu, *TeV gravity in four dimensions?*, *Phys. Lett. B* **663** (2008) 95–98, [[arXiv:0711.2306v1 \[hep-th\]](#)].
- [6] X. Calmet, S. D. H. Hsu, and D. Reeb, *Quantum gravity at a TeV and the renormalization of Newton’s constant*, *Phys. Rev. D* **77** (2008) 125015, [[arXiv:0803.1836v2 \[hep-th\]](#)].
- [7] P. C. Argyres, S. Dimopoulos, and J. March-Russell, *Black holes and sub-millimeter dimensions*, *Phys. Lett. B* **441** (1998) 96–104, [[arXiv:hep-th/9808138v1](#)].
- [8] T. Banks and W. Fischler, *A model for high energy scattering in quantum gravity*, 1999. [[arXiv:hep-th/9906038v1](#)].
- [9] S. B. Giddings and S. Thomas, *High energy colliders as black hole factories: The end of short distance physics*, *Phys. Rev. D* **65** (2002) 056010, [[arXiv:hep-ph/0106219v4](#)].
- [10] **Particle Data Group** Collaboration, W.-M. Yao *et al.*, *Review of particle physics*, *J. Phys. G* **33** (2006) 1.
- [11] D. J. Kapner, T. S. Cook, E. G. Adelberger, J. H. Gundlach, B. R. Heckel, C. D. Hoyle, and H. E. Swanson, *Tests of the gravitational inverse-square law below the dark-energy length scale*, *Phys. Rev. Lett.* **98** (2007) 021101, [[arXiv:hep-ph/0611184v1](#)].
- [12] A. Heister *et al.* (ALEPH Collaboration), *Single- and multi-photon production in e^+e^- collisions at \sqrt{s} up to 209 GeV*, *Eur. Phys. J. C* **28** (2003) 1–13.
- [13] J. Abdallah *et al.* (DELPHI Collaboration), *Photon events with missing energy in e^+e^- collisions at $\sqrt{s} = 130$ to 209 GeV*, *Eur. Phys. J. C* **38** (2005) 395–422, [[arXiv:hep-ex/0406019v2](#)].
- [14] P. Achard *et al.* (L3 Collaboration), *Single- and multi-photon events with missing energy in e^+e^- collisions at LEP*, *Phys. Lett. B* **587** (2004) 16–32, [[arXiv:hep-ex/0402002v1](#)].
- [15] LEP Exotica Working Group, ALEPH, DELPHI, L3, and OPAL Collaborations, *Combination of LEP results on direct searches for large extra dimensions*, 2004. CERN Note LEP Exotica WG 2004-03.
- [16] A. Abulencia *et al.* (CDF Collaboration), *Search for large extra dimensions in the production of jets and missing transverse energy in $p\bar{p}$ collisions at $\sqrt{s} = 1.96$ TeV*, *Phys. Rev. Lett.* **97** (2006) 171802, [[arXiv:hep-ex/0605101v1](#)].
- [17] V.M. Abazov *et al.* (DØ Collaboration), *Search for large extra dimensions in the mono-photon final state at $\sqrt{s} = 1.96$ TeV*, *Phys. Rev. Lett.* **101** (2008) 011601, [[arXiv:0803.2137v2 \[hep-ex\]](#)].

- [18] S. Hannestad and G. G. Raffelt, *Supernova and neutron-star limits on large extra dimensions reexamined*, *Phys. Rev. D* **67** (2003) 125008, [[arXiv:hep-ph/0304029v2](#)].
- [19] S. Hannestad and G. G. Raffelt, *Erratum: Supernova and neutron-star limits on large extra dimensions reexamined*, *Phys. Rev. D* **69** (2004) 029901, [[arXiv:hep-ph/0304029v2](#)].
- [20] M. Fairbairn, *Cosmological constraints on large extra dimensions*, *Phys. Lett. B* **508** (2001) 335–339, [[arXiv:hep-ph/0101131v3](#)].
- [21] M. Fairbairn and L. M. Griffiths, *Large extra dimensions, the galaxy power spectrum and the end of inflation*, *J. High Energy Physics* **02** (2002) 024, [[arXiv:hep-ph/0111435v3](#)].
- [22] N. Kaloper, J. March-Russell, G. D. Starkman, and M. Trodden, *Compact hyperbolic extra dimensions: Branes, Kaluza-Klein modes and cosmology*, *Phys. Rev. Lett.* **85** (2000) 928–931, [[arXiv:hep-ph/0002001v1](#)].
- [23] M. Cassé, J. Paul, G. Bertone, and G. Sigl, *Gamma rays from the galactic bulge and large extra dimensions*, *Phys. Rev. Lett.* **92** (2004) 111102, [[arXiv:hep-ph/0309173v2](#)].
- [24] L. A. Anchordoqui, J. L. Feng, H. Goldberg, and A. D. Shapere, *Black holes from cosmic rays: Probes of extra dimensions and new limits on TeV-scale gravity*, *Phys. Rev. D* **65** (2002) 124027, [[arXiv:hep-ph/0112247v3](#)].
- [25] L. A. Anchordoqui, J. L. Feng, H. Goldberg, and A. D. Shapere, *Updated limits on TeV-scale gravity from the absence of neutrino cosmic ray showers mediated by black holes*, *Phys. Rev. D* **68** (2003) 104025, [[arXiv:hep-ph/0307228v1](#)].
- [26] S. Dimopoulos and G. Landsberg, *Black holes at the Large Hadron Collider*, *Phys. Rev. Lett.* **87** (2001) 161602, [[arXiv:hep-ph/0106295v1](#)].
- [27] D. M. Gingrich and K. Martell, *Study of highly-excited string states at the Large Hadron Collider*, *Phys. Rev. D* **78** (2008) 115009, [[arXiv:0808.2512v3 \[hep-ph\]](#)].
- [28] X. Calmet, W. Gong, and S. D. H. Hsu, *Colorful quantum black holes at the LHC*, *Phys. Lett. B* **668** (2008) 20–23, [[arXiv:0806.4605v2 \[hep-th\]](#)].
- [29] P. Meade and L. Randall, *Black holes and quantum gravity at the LHC*, *J. High Energy Physics* **05** (2008) 003, [[arXiv:0708.3017v1 \[hep-ph\]](#)].
- [30] K. S. Thorn, *Nonspherical gravitational collapse: A short review*, 2002. in J. R. Klauder, Magic Without Magic, San Francisco.
- [31] J. A. Frost, J. R. Gaunt, M. O. P. Sampaio, M. Casals, S. R. Dolan, M. A. Parker, and B. R. Webber, *Phenomenology of production and decay of spinning extra-dimensional black holes at hadron colliders*, *J. High Energy Physics* **10** (2009) 014, [[arXiv:0904.0979v4 \[hep-ph\]](#)].
- [32] D. M. Gingrich, *Black hole cross-section at the LHC*, *Int. J. Mod. Phys. A* **21** (2006) 6653–6676, [[arXiv:hep-ph/0609055v2](#)].
- [33] D. M. Eardley and S. B. Giddings, *Classical black hole production in high-energy collisions*, *Phys. Rev. D* **66** (2002) 044011, [[arXiv:gr-qc/0201034v2](#)].
- [34] H. Yoshino and Y. Nambu, *Black hole formation in the grazing collision of high-energy particles*, *Phys. Rev. D* **67** (2003) 024009, [[arXiv:gr-qc/0209003v1](#)].
- [35] H. Yoshino and V. S. Rychkov, *Improved analysis of black hole formation in high-energy particle collisions*, *Phys. Rev. D* **71** (2005) 104028, [[arXiv:hep-th/0503171v2](#)].

- [36] H. Yoshino and R. B. Mann, *Black hole formation in the head-on collision of ultrarelativistic charges*, *Phys. Rev. D* **74** (2006) 044003, [[arXiv:gr-qc/0605131v3](#)].
- [37] D. M. Gingrich, *Effect of charged partons on black hole production at the Large Hadron Collider*, *J. High Energy Phys.* **02** (2007) 098, [[arXiv:hep-ph/0612105v3](#)].
- [38] H. Yoshino, A. Zelnikov, and V. P. Frolov, *Apparent horizon formation in the head-on collision of gyratons*, *Phys. Rev. D* **75** (2007) 124005, [[arXiv:gr-qc/0703127v3](#)].
- [39] E. Kohlprath and G. Veneziano, *Black holes from high-energy beam-beam collisions*, *J. High Energy Phys.* **06** (2002) 057, [[arXiv:gr-qc/0203093v2](#)].
- [40] S. N. Solodukhin, *Classical and quantum cross-section for black hole production in particle collisions*, *Phys. Lett. B* **533** (2002) 153–161, [[arXiv:hep-ph/0201248v2](#)].
- [41] S. D. H. Hsu, *Quantum production of black holes*, *Phys. Lett. B* **555** (2003) 92–98, [[arXiv:hep-ph/0203154v2](#)].
- [42] J. Pumplin, D. Stump, J. Huston, H. L. Lai, P. Nadolsky, and W. K. Tung, *New generation of parton distributions with uncertainties from global QCD analysis*, *J. High Energy Phys.* **07** (2002) 012, [[arXiv:hep-ph/0201195v3](#)].
- [43] S. W. Hawking, *Particle creation by black holes*, *Commun. math. Phys.* **43** (1975) 199–220.
- [44] C. M. Harris and R. Kanti, *Hawking radiation from a $(4+n)$ -dimensional black hole: Exact results for the Schwarzschild phase*, *J. High Energy Phys.* **10** (2003) 014, [[arXiv:hep-ph/0309054v2](#)].
- [45] V. Cardoso, M. Cavaglià, and L. Gualtieri, *Hawking emission of gravitons in higher dimensions: Non-rotating black holes*, *J. High Energy Phys.* **02** (2006) 021, [[arXiv:hep-th/0512116v3](#)].
- [46] C. M. Harris, *Physics Beyond the Standard Model: Exotic Leptons and Black Holes at Future Colliders*. PhD thesis, University of Cambridge, December, 2003. [arXiv:hep-ph/0502005v1](#).
- [47] J. D. Bekenstein and V. F. Mukhanov, *Spectroscopy of the quantum black hole*, *Phys. Lett. B* **360** (1995) 7–12, [[arXiv:gr-qc/9505012v1](#)].
- [48] D. M. Gingrich, *Monte Carlo event generator for quantum black hole production and decay in proton-proton collisions*, 2009. [arXiv:0911.5370v1](#) [hep-ph].
- [49] T. Sjöstrand, S. Mrenna, and P. Skands, *A brief introduction to PYTHIA 8.1*, *Comput. Phys. Commun.* **178** (2008) 852–867, [[arXiv:0710.3820v1](#)].
- [50] T. Sjöstrand, S. Mrenna, and P. Skands, *PYTHIA 6.4 physics and manual*, *J. High Energy Phys.* **0605** (2006) 026, [[arXiv:hep-ph/0603175v2](#)].